High-resolution core-level study of the (100), (110), and (111) surfaces of Cr_3Si

K. L. Håkansson and L. I. Johansson
Department of Physics and Measurement Technology, Linköping University, S-581 83 Linköping, Sweden

A. N. Christensen
Department of Chemistry, Aarhus University, DK-8000 Aarhus C, Denmark
(Received 24 February 1992)

High-resolution angle-resolved photoemission investigations of core levels of the (100), (110), and (111) surfaces of Cr_3Si have been performed using synchrotron radiation. Surface-shifted Si $2p$ levels were observed on all three surfaces, but no shifted Cr $3p$ levels could be identified. The core-level shifts were extracted using a curve-fitting procedure, and it was found necessary to use two surface-shifted components for each surface. Shifts of -0.29 and -0.56 eV for the (100) surface, of -0.42 and -0.77 eV for the (110) surface, and of -0.27 and $+0.28$ eV for the (111) surface were extracted. The reaction rate for these surfaces upon oxygen exposure was investigated, and significant differences were observed. The (100) surface was found to show the highest reaction rate and the (110) surface the lowest. Initial Si oxidation was observed on all three surfaces, while Cr oxidation could be revealed only after higher oxygen doses. Clear diffraction effects were observed in the Si $2p$ surface-to-bulk intensity ratio both as a function of electron emission angle and photoelectron kinetic energy. These results are presented and discussed.

I. INTRODUCTION

The electronic properties of transition-metal silicides have attracted considerable interest during the past decade.[1,2] The formation of silicides in transition-metal–silicon interfaces produces rather stable silicide-silicon interfaces and clean contacts[2] which have important applications in semiconductor industry.[1,2] Different phases of silicides can, however, be formed in such reactions, so data from bulk silicide crystals are often required for drawing firm conclusions about, for example, the growth mode and silicide stoichiometry at the interface. Several studies have been reported earlier on reacted Cr/Si interfaces and of polycrystalline chromium silicides,[3–9] but only one[10] of a single-crystal sample. Therefore we have continued investigations of the low-index surfaces of a chromium silicide single crystal.

Angle-resolved photoemission studies of the (100), (110), and (111) surfaces of a Cr_3Si single crystal have been performed in order to investigate the electronic structure and possible geometry at the surfaces. In this article high-resolution core-level results from the three clean surfaces, prepared *in situ* by sputter and annealing cycles, are presented. Effects induced in the core-level spectra upon oxygen exposure are also presented and discussed. Surface-shifted Si $2p$ levels are observed on all three surfaces, but no shifted Cr $3p$ levels can be identified. It was found necessary to use two surface-shifted components for all three surfaces in order to model the recorded spectra. For the (100) and (110) surfaces both components are shifted towards lower binding energy, while for the (111) surface there is one shift in each direction. The oxygen-induced effects indicate a rapid initial oxidation of Si, while higher oxygen exposures are found to be needed in order to observe a chemically shifted Cr $3p$ peak. These findings are presented and discussed.

II. EXPERIMENTAL DETAILS

The experiments were performed at the synchrotron radiation facility MAX Laboratory in Lund. The beam line utilized is equipped with a toroidal grating monochromator[11] having three interchangeable gratings and producing photons with energies between 15 and 200 eV. The photon energy resolution is dependent on the operation parameters, but was for the high-resolution studies of the Si $2p$ core levels chosen to be less than 0.2 eV. The hemispherical electron analyzer has an acceptable angle of $\pm 2°$ and was typically operated at an energy resolution of less than 0.1 eV.

The growth method used to produce monocrystal rods of Cr_3Si has been described earlier.[10] Crystals having the (100), (110), and (111) orientation were spark cut from the monocrystal rod and mechanically polished. The orientation was checked by Laue patterns to be within $\pm 1°$. The crystals were cleaned *in situ* by a short Ar^+-ion bombardment (20 mA at 2000 V$\approx$2 min and then at 500 V$\approx$3 min) followed by repeated short annealings to a temperature of around 800 °C for the (100) surface, 1000 °C for the (110) surface, and 1100 °C for the (111) surface. The cleaning procedures were checked using Auger electron spectroscopy (AES) and low-energy electron diffraction (LEED) to produce clean and well-ordered surfaces. A constant Si-to-Cr signal ratio was obtained in the AES spectra after a few annealings. Distinct 1×1 LEED patterns were observed from the (110) and (111) surfaces. For the (100) surface the pattern was found to include weaker superstructure spots as shown in Fig. 1(a). We suggest these to originate from a two domain

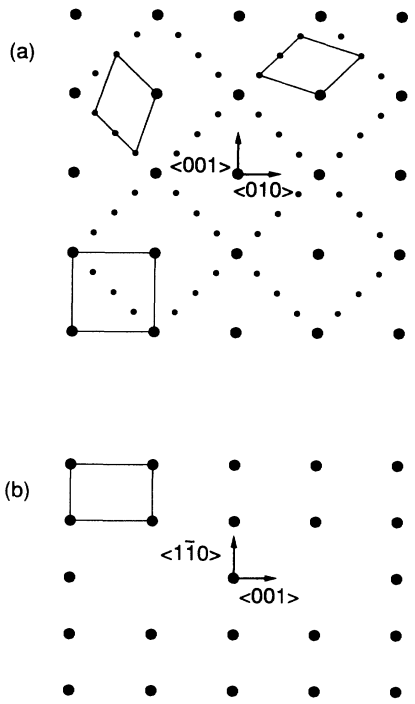

FIG. 1. Illustration of the observed LEED patterns from (a) the (100) surface and (b) the (110) surface.

$c(\sqrt{2}\times 2\sqrt{2})R45°$ overlayer structure as discussed below. For comparison the LEED pattern observed on the (110) surface is illustrated in Fig. 1(b). The LEED patterns were used to set the desired azimuthal directions which were $\langle 011\rangle$, $\langle 001\rangle$, and $\langle 01\bar{1}\rangle$ for the (100), (110), and (111) surface, respectively. Oxygen exposures were made at room temperature at pressures in the 10^{-8}–10^{-5} Torr range. The base pressure in the spectrometer was 2×10^{-10} Torr. The exposure is given as the total pressure read at the ion gauge times the exposure time ($1\ \mathrm{L}=10^{-6}$ Torr s). All measurements were performed at room temperature.

III. RESULTS

High-resolution Si $2p$ spectra recorded at a photon energy of 130 eV from the (100), (110), and (111) surfaces at normal emission are shown by the dotted curves in Figs. 2(a)–2(c), respectively. An integrated background has been subtracted to compensate for the effects of inelastically scattered electrons. Surface-shifted components are needed in order to model the recorded spectra for all three surfaces. The results of a curve-fitting procedure[12] are shown by the solid lines through the data points in the figure. The fitted components are shown as shaded curves, where the darkest component corresponds to the bulk component and the lighter ones to the surface components. The parameters often used for fitting Si $2p$ spectra have been utilized in these fits, i.e., a spin-orbit split of 0.61 eV, a branching ratio of 0.5, and a Lorentzian full width at half maximum (FWHM) of 0.07 eV. Asymmetry parameter values of 0.12 for the surface shifted components and 0.00 for the bulk component were selected from the best fits of the (110) spectra, where the surface shifts are largest and the fits are easiest to make; see Fig. 2(b). These asymmetry parameter values were then used also for the two other surfaces and are actually the values found earlier to produce the best fits of Si $2p$ spectra from Mo_3Si (100) and (110).[13] A Gaussian (instrumental) FWHM of 0.24(±0.01) eV was used for the spectra shown in Fig. 2. For determining the surface shifts normal emission spectra recorded at photon energies between 108 and 140 eV have been analyzed. The values given below in parentheses represent the maximum spread in the results of the curve fitting using all relevant recorded spectra.

Of the three surfaces studied the (110) surface is the easiest to analyze since it exhibits two clearly resolved surface-shifted components. The fitting procedure resulted in this case in surface core-level shifts of $-0.42(\pm 0.02)$ eV and $-0.77(\pm 0.02)$ eV relative to the binding energy of the bulk Si $2p_{3/2}$, which was determined to be $98.9(\pm 0.1)$ eV. For the (100) surface the

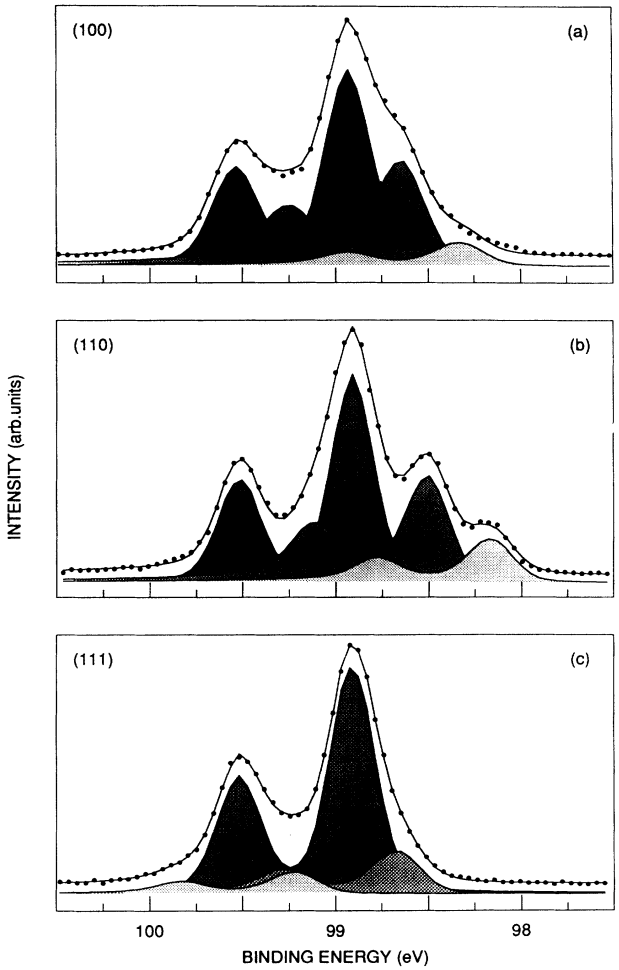

FIG. 2. Si $2p$ core-level spectra recorded at normal emission from (a) the (100) surface, (b) the (110) surface, and (c) the (111) surface using a photon energy of 130 eV. The dotted curves show the recorded data points, the solid curves represent the result of the curve fitting procedure, and the shaded curves show the extracted bulk (dark) and surface shifted (lighter) components.

question was raised in an earlier article of Cr_3Si (100) (Ref. 10) if the Si 2*p* spectrum has one quite broad surface-shifted component or two narrower components. Judging from the fits made this time, using the same spectra as in that article and the fitting parameters from the (110) surface, the answer to this is that there are at least two shifted components. Surface shifts of $-0.30(\pm 0.01)$ and $-0.58(\pm 0.04)$ eV are extracted when using two shifted components. The fit obtained at the foot on the low binding energy side is, however, not really satisfactory. One could therefore even consider the possibility that there is a third shifted component. When using three surface components shifts of $-0.28(\pm 0.01)$, $-0.52(\pm 0.03)$, and $-0.82(\pm 0.02)$ eV are extracted. Since the relative intensity of the component having the largest shift becomes very weak, less than 5% of the bulk component, and since fits of comparable quality are obtained when using two shifted components we can, however, only conclude that there are at least two shifted components for the (100) surface having shifts of $-0.29(\pm 0.02)$ and $-0.56(\pm 0.06)$ eV. The Si 2*p* spectrum from the (111) surface appears at first sight to contain only a bulk component. When trying to fit this spectrum it was, however, not possible to get a reasonably good fit using only a bulk component. When using the same parameters as for the other two surfaces it was in fact found necessary to use two surface components and shifts of $-0.27(\pm 0.02)$ and $+0.28(\pm 0.02)$ eV were obtained, i.e., shifts having the same size but different signs. Only this surface exhibits a surface component shifted towards higher binding energy.

For the main purpose of investigating the reactivity, but also for identifying surface shifted components, these three surfaces were exposed to different amounts of oxygen. Si 2*p* spectra recorded after different exposures using a photon energy of 130 eV are shown in Fig. 3. Large differences in the oxidation rate for the different surfaces are clearly observed. For the (100) surface the Si 2*p* spectrum is clearly affected at an oxygen dose of 3 L (1 $L = 10^{-6}$ Torr s) and a silicon oxide related peak[14] is observed at around 3.7 eV higher binding energy; see Fig. 3(a). This peak can in fact be observed, although very weak, already in the 1-L spectrum. In comparison the (110) and (111) surfaces are initially much less affected by oxygen since exposures of 30 L are needed in order to observe oxide related peaks; see Figs. 3(b) and 3(c). The least reactive of the three surfaces is seen to be the (110) since the relative intensity of the oxide-related peak observed at an exposure of 30 L is much smaller than for the (111) surface. Even at an oxygen dose of 300 L bulk Si 2*p* peaks are still seen fairly clearly in the (110) spectrum, while they have disappeared almost completely for the other two surfaces. The previously discussed surface-shifted components are found to be more affected upon oxidation than the corresponding bulk peaks which support the assignments made above.

Chromium spectra have also been recorded for the purpose of revealing surface-shifted Cr 3*p* levels and how these levels are affected upon oxygen exposures. Cr 3*p* spectra recorded from the clean surfaces are shown by the bottom curves in Figs. 4(a), 4(b), and 4(c), respectively. These spectra look, after background subtraction, identical for all three surfaces. This was also checked using the curve-fitting program by which it was possible to subtract spectra from each other after normalization and the difference spectrum obtained was a straight line

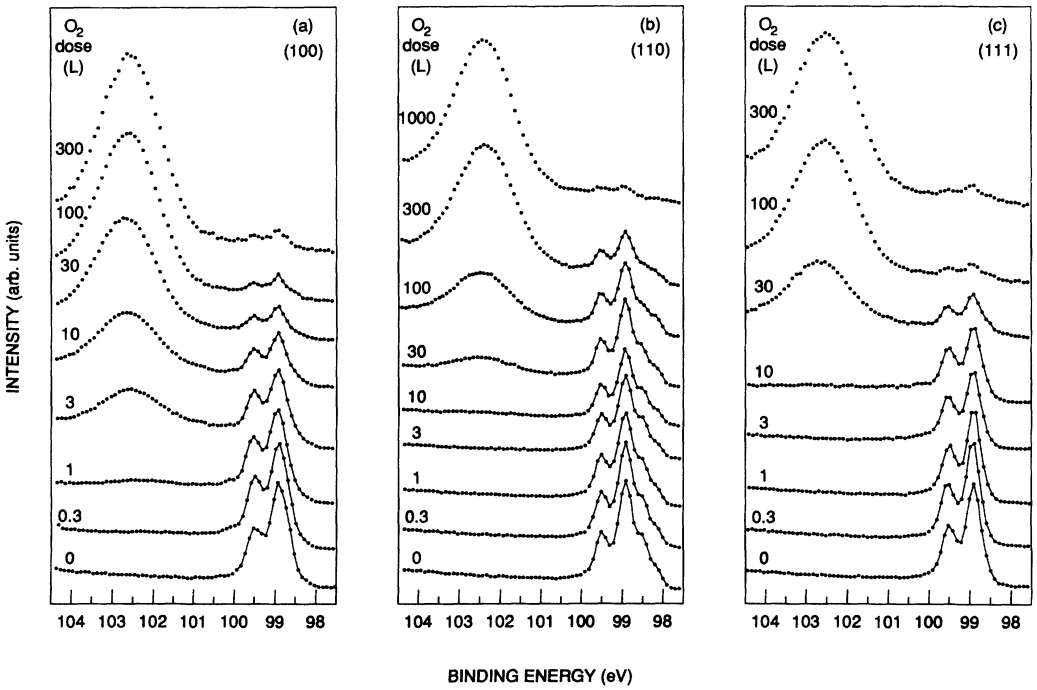

FIG. 3. Si 2*p* spectra recorded at normal emission after different oxygen exposures using a photon energy of 130 eV from (a) the (100) surface, (b) the (110) surface, and (c) the (111) surface.

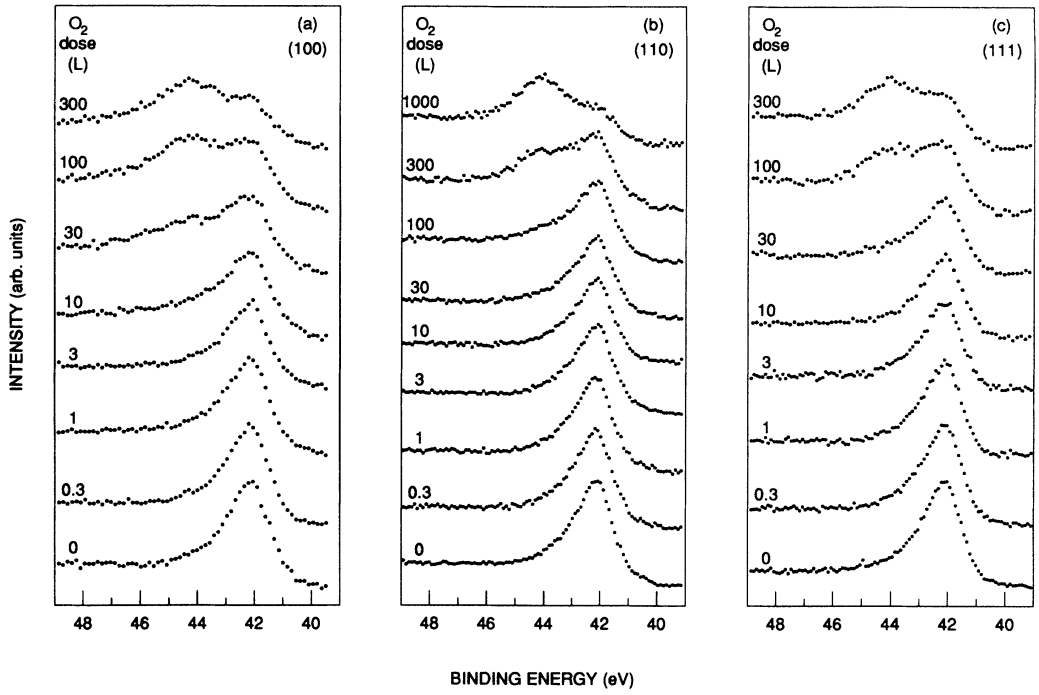

FIG. 4. Cr $3p$ spectra recorded at normal emission after different oxygen exposures from (a) the (100) surface, (b) the (110) surface, and (c) the (111) surface. In (a) a photon energy of 110 eV was used, while 118 eV was used in (b) and (c).

without any structures. The result was the same if the difference was taken between spectra from different surfaces and/or at different emission angles ($\theta_e = 0°$ and 50° were used). The conclusion must therefore be the same for the (110) and (111) surfaces as for the (100) surface presented earlier.[10] No surface-shifted core levels can be identified in the Cr $3p$ spectrum for any of the three surfaces studied. Upon oxygen exposures a similar difference in oxidation rate between the different surfaces can be observed in the Cr $3p$ spectra as discussed earlier

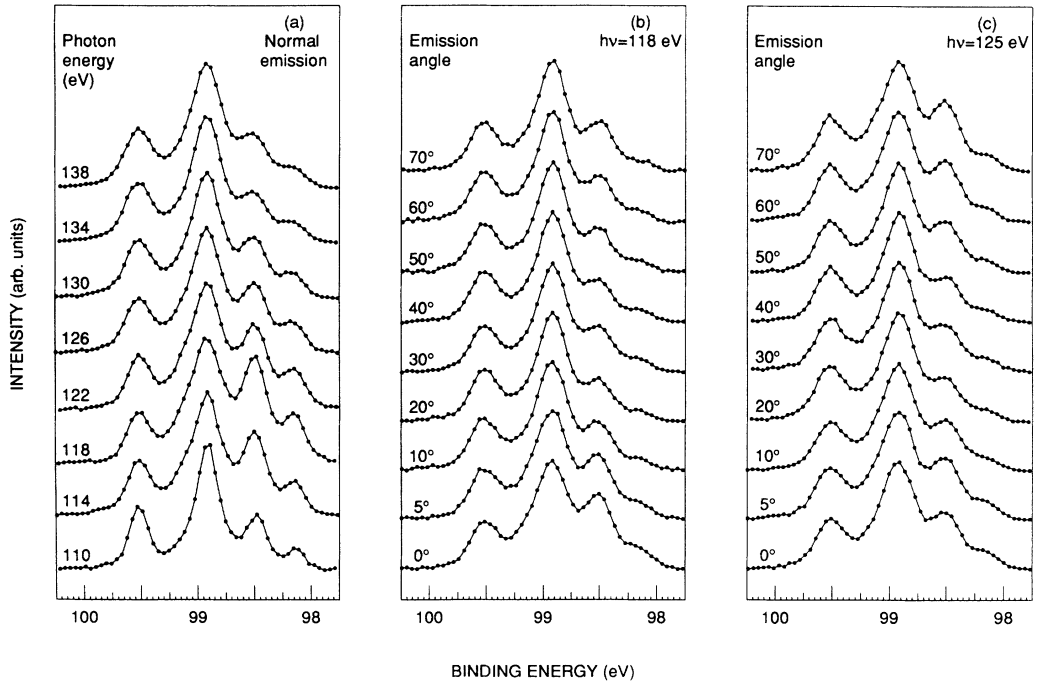

FIG. 5. Si $2p$ spectra from the (110) surface recorded (a) at normal emission using different photon energies, (b) and (c) at different emission angles using two different photon energies.

for the Si $2p$ spectra; see Fig. 4. The oxide-related peak, at approximately 2 eV higher binding energy,[10,15] appears, however, at higher doses of oxygen in the Cr $3p$ spectra than in the Si $2p$ spectra, indicating an initial rapid silicon oxidation. This difference in the oxidation rate, initial Si oxidation, and appearance of a metal oxide peak at much larger exposures, if observed at all, has been reported earlier for other transition metal silicides.[13,16–19]

Distinct diffraction effects have been observed in the surface-to-bulk intensity ratio in earlier experiments on transition metal silicides[13,20] both as a function of photoelectron kinetic energy and electron emission angle. Such effects were observed also in this investigation and most pronounced for the (110) surface which is illustrated in Fig. 5. Normal emission spectra recorded at different photon energies are shown in Fig. 5(a) and spectra recorded at different electron emission angles along the ⟨001⟩ azimuth using two different photon energies, 118 and 125 eV, are shown in Figs. 5(b) and 5(c). In order to better illustrate the diffraction effects the extracted surface to bulk intensity ratios for the major surface shifted component have been plotted in Fig. 6. The extracted ratio is shown as a function of photon energy in Fig. 6(a) and as a function of electron emission angle in Fig. 6(b). The ratios extracted in the normal emission spectra for the (100) and (111) surfaces are also included in Fig. 6(a). Neglecting diffraction effects the ratio versus photon energy should exhibit a maximum where the energy dependent mean free path has its minimum which occurs around a kinetic energy of about 25 eV,[21] corresponding to a photon energy around 130 eV. For the (100) surface the extracted ratio is seen to show this behavior; see Fig. 6(a). The result for the (110) surface is, however, quite different, showing a maximum around a photon energy of 118 eV and a minimum around 134 eV. A similar behavior is observed also for the (111) surface, although the extracted ratios are considerably smaller in this case. When varying the emission angle the surface-to-bulk intensity ratio should increase monotonically[20] with increasing emission angle if diffraction effect can be neglected. The experimental results show, however, a quite different behavior; see Fig. 6(b). At a photon energy of 118 eV the ratio is actually largest at normal emission [squares in Fig. 6(b)] and decreases with increasing emission angle up to about $\theta_e = 20°$. Between $\theta_e = 20°$ and 40° it exhibits a local maximum, but thereafter it shows a slow increase with emission angle. The result for $h\nu = 125$ eV is quite similar, the main differences being a more pronounced increase at large emission angles and an increase the first 5°. These results clearly show that diffraction effects must be included in an interpretation of the surface-to-bulk intensity ratios.

IV. DISCUSSION

Can formation of silicides with a different composition in the surface region explain the shifted components? A Si $2p_{3/2}$ binding energy of 98.9 eV was determined for the bulk component in Cr_3Si, while binding energies of 99.0 and 99.5 eV have been reported earlier for CrSi and $CrSi_2$, respectively.[3,7] A chemical shift towards higher binding energy is thus expected for both CrSi and $CrSi_2$,

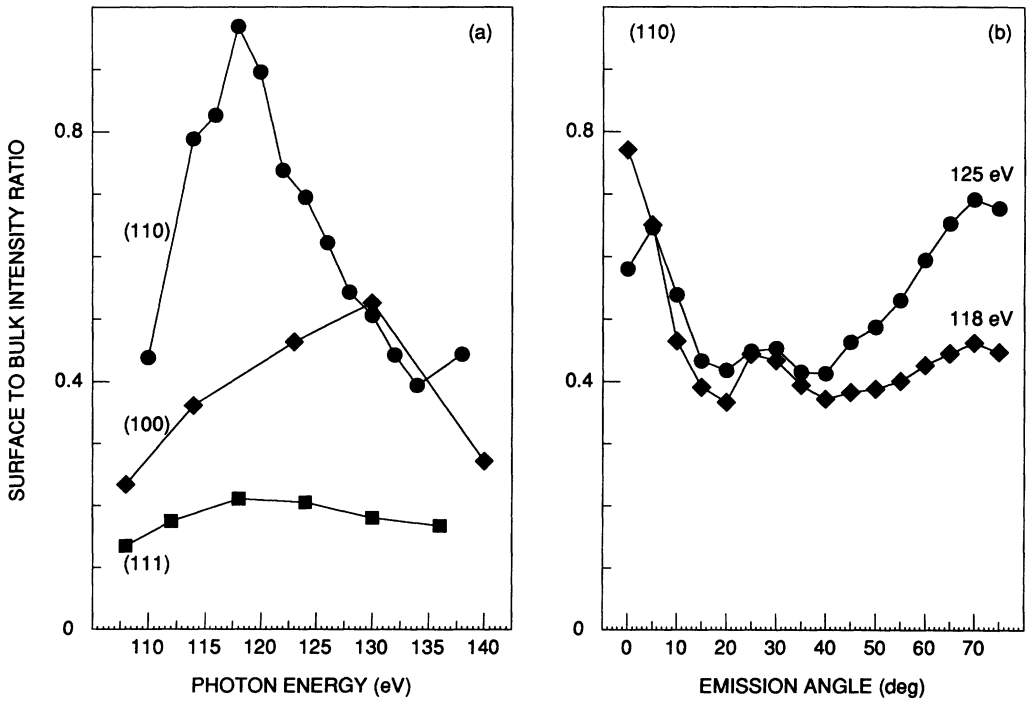

FIG. 6. Extracted surface to bulk intensity ratio for the Si $2p$ levels (a) as a function of photon energies for the different surfaces and (b) as a function of emission angle for the (110) surface using two different photon energies. That the ratios extracted for the (110) surface at normal emission in (b) are somewhat smaller than those in (a) is probably partly due to the fact that latter data were recorded much later in the experiment so several annealings had been made in between these recordings.

while the components observed in general are shifted towards lower binding energy. The exception being the weakest component on the (111) surface, which is shifted towards higher binding energy, but its binding energy does not match the binding energies of these silicides. Formation of these types of silicides in the surface region can therefore not provide an explanation of the shifted levels observed.

In seeking an explanation to the origin of the surface-shifted core levels and to the different reactivities observed upon oxygen exposures it is worthwhile to consider how the different surfaces may be terminated. We first look for possibilities to obtain Si in the surface layer when truncating the bulk structure since surface shifted Si $2p$ levels were observed on all three surfaces investigated and since the effects induced in the core levels upon oxygen exposures, a rapid initial Si oxidation and Cr oxidation at larger exposures, also suggest presence of Si in the surface layer. The unit cell of Cr_3Si is shown in Fig. 7(a). It consists of Si atoms in bcc positions with pairs of Cr atoms located in perpendicular directions on neighboring faces of the cube. This means that in the $\langle 110 \rangle$ direction every fourth plane contains only Si atoms while the three planes in between only Cr. The concentration of atoms is the same in each layer and the interlayer distance is $a/4\sqrt{2}$, where a is the lattice parameter [4.56 Å (Ref. 7)]. Assuming Si as the terminating layer for the (110) surface results in the model shown in Fig. 7(b). The LEED pattern from this surface, shown in Fig. 1(b), is possible to obtain by just summing the diffraction patterns from at least the first two layers.

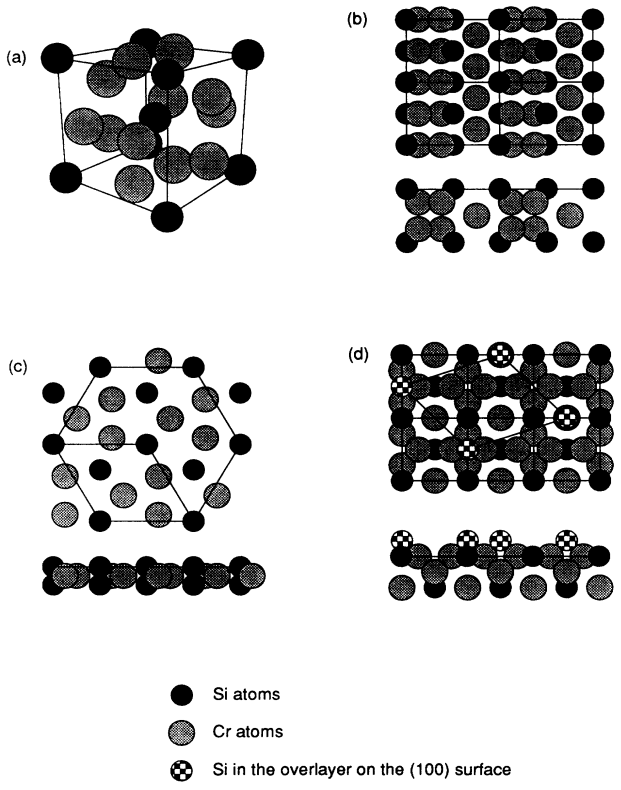

FIG. 7. (a) The unit cell of Cr_3Si where the large gray circles represents Cr atoms and the small black circles represents Si atoms. The top and side view of the low index surfaces are shown in (b)–(d) when assuming perfect bulk termination with Si in the surface layer for the (110) and (111) surfaces and a Si overlayer for the (100) surface.

For the $\langle 111 \rangle$ direction in the unit cell every second plane contains only Si atoms and the plane in between only Cr, with an atom concentration three times higher than in the Si plane. The interlayer distance is $a/4\sqrt{3}$. Assuming Si termination also for the (111) surface results in the model shown in Fig. 7(c). It is thus possible to obtain a single terminating Si layer on the (110) and (111) surfaces by just truncating the bulk structure. We cannot, of course, exclude the possibility that these surfaces have overlayer structures that are compatible with the diffraction patterns from the bulk layers.

For the $\langle 100 \rangle$ direction in the unit cell every second plane contains both types of atoms while the planes in between contain only Cr atoms. In the mixed layer the concentration of Cr atoms is twice the Si concentration and in the Cr layer the concentration is the same as for Si in the mixed layer. The interlayer distance is $a/4$. Perfect bulk termination can, however, be excluded for this surface since it would result in a quadratic LEED pattern and that is not observed as seen in Fig. 1(a). It should be noted that the LEED pattern from the (100) surface was misinterpreted in our earlier investigation on Cr_3Si.[10] The large filled circles in Fig. 1(a) illustrate the 1×1 LEED pattern and the small filled circles the superstructure spots. The pattern of the superstructure spots can be constructed by two identical oblique (primitive) unit meshes rotated 90° compared to each other and with their short sides rotated 45° compared to the sides of the 1×1 primitive mesh. The two oblique unit meshes and the quadratic unit mesh are shown in Fig. 1(a). The area of the oblique mesh is half the area of the quadratic mesh, which means that the oblique unit mesh in the real space is twice as large as the quadratic unit mesh. The simplest way to construct the origin to this LEED pattern is by using a two-domain oblique overlayer structure on the truncated crystal. This overlayer structure can also be viewed as a two-domain $c(\sqrt{2}\times2\sqrt{2})R45°$ structure using Wood's notations.[22] We cannot, of course, eliminate the possibility of a more complex overlayer structure such as coexistence of both domains in the same area. This would, however, imply twice as many Si atoms in the surface layer, but the relative intensity in the surface-shifted levels do not appear to be large enough to account for that.[21] If the (100) surface is assumed to be terminated with the discussed oblique overlayer structure on a mixed plane, the structural model shown in Fig. 7(d) can be obtained for one of the domains where the square and the oblique unit meshes corresponding to the ones in Fig. 1(a) are marked. The positions of the atoms in the overlayer structure cannot be determined from the LEED pattern, but have in Fig. 7(d) been chosen as two different bridge sites relative to the Si sites in the mixed layer. When trying various possibilities these overlayer atoms will in general occupy two inequivalent positions, but it is possible to find equivalent positions, although

these seem more unlikely.

By assuming perfect bulk termination for the (110) and (111) surfaces and an overlayer structure for the (100) surface it is thus possible to obtain Si termination on all three surfaces. For the (100) surface at least two surface-shifted Si components can be anticipated especially if the Si overlayer atoms occupy two inequivalent positions. For the (110) and (111) surfaces the atoms in the terminating Si layer will, however, experience the same surrounding and the suggested models can therefore explain the appearance of one surface shifted Si level but not the occurrence of two shifted components, which is further discussed below. First we consider what implications these models have concerning the surface reactivities.

Large differences in the oxidation rate were observed between the three surfaces investigated and similar differences have been observed earlier between the (100) and (110) surfaces of Mo_3Si.[13] For nickel and palladium silicides large increases in the oxidation rate were observed[18,19] for increasing metal concentration in the compositions. It was suggested[19] that the metal atoms act as a catalyst to dissociate the molecular oxygen in more reactive atomic oxygen. This provided an explanation why the silicides are much more reactive than pure silicon[23] and also why the oxidation rate increased with increasing metal concentration. Based on this we would expect the surface having the highest concentration of Cr in the surface region to be most reactive towards oxygen. The models suggested in Fig. 7 have all a surface layer consisting of Si and a second layer containing Cr. The (100) surface, which was found to be the most reactive, has the lowest density of Si in the topmost layer (0.5 Si atoms/a^2, where a is the lattice parameter) and the highest density of Cr in the second (mixed) layer (2 Cr atoms/a^2). The (111) surface, which was found to be less reactive, has a slightly higher Si density in the surface layer ($1/\sqrt{3} \approx 0.6$ Si atoms/a^2) and the second layer contains also less Cr ($\sqrt{3} \approx 1.7$ Cr atoms/a^2) than the (100) surface. Finally the (110) surface, which was found to be least reactive, has the highest density of Si in the surface layer ($\sqrt{2} \approx 1.4$ Si atoms/a^2) and the lowest density of Cr in the second layer ($\sqrt{2} \approx 1.4$ Cr atoms/a^2) of the three surfaces. The experimental observations and the surface models proposed are thus in agreement with the suggestion that the metal atoms dissociate the oxygen molecules and increase the reaction rate.

A thermochemical model,[24] in which the total shift is expressed as a sum of partial shifts, has been used earlier to estimate surface shifts on alloys[24] and compounds.[13] For Cr_3Si,[10] this model predicts that total loss of coordination at the surface would result in a surface shift of -0.38 eV. For perfect bulk terminated (110) and (111) surfaces the number of nearest neighbors for the Si surface atoms are reduced from twelve to six, predicting a shift of -0.19 eV. If the (100) surface would be bulk terminated, a shift of $\frac{2}{3}$ of that value would be predicted. This was discussed in an earlier investigation[13] of the (100) and (110) surfaces of Mo_3Si and the relative size of the shifts for the major surface components were in that investigation found to have that relation. In view of the present results that finding must, however, be considered to be fortuitous since the model predicts the same shift for the (110) and (111) surfaces while different shifts are found experimentally. Negative shifts are observed for the major surface components on all three Cr_3Si surfaces investigated and are also predicted by this model, but other factors than the effective coordination at the surface seem to be of importance for the size of the surface shift.

The second surface-shifted component on the (110) and (111) surfaces cannot be explained by the structural models proposed in Fig. 7. Therefore one may speculate about their origin. Can they, for example, arise from an extra Si layer diffused to the surface during the annealing or from relaxation effects. A supporting argument for the former is that it was observed in an earlier Auger experiment on $V_3Si(100)$ (Ref. 16) that the intensity ratio between V and Si decreased during the annealing when superstructure spots started to appear in the LEED pattern. We could on the contrary not observe any changes in the Cr-to-Si Auger signal ratio upon annealings after an ordered surface had been obtained as checked by LEED, but this does not exclude the possibility of surface diffusion before an ordered surface was formed. For the (100) surface the LEED pattern shown in Fig. 1(a) was obtained and we could not observe a 1×1 pattern at lower annealing temperatures. However, since the structural model proposed in that earlier study must have been misdrawn [see Figs. 2(b) and 2(c) in Ref. 16] and since the LEED pattern observed was not shown, we are uncertain if the reconstruction observed on $V_3Si(100)$ was different from the one we observe on $Cr_3Si(100)$. For $CoSi_2(111)$ it has also been shown that sputtered and annealed single-crystal surfaces are Si rich compared to cleaved surfaces.[20,25] For both $CrSi_2$ and $CoSi_2$ it was shown that the intensity of the surface silicon component increases with increasing annealing temperature[7,26] indicating diffusion of Si to the surface. In general results on transition-metal silicide bulk crystals show that the surfaces are Si terminated,[20,23–28] but questions have been raised whether it is a single layer or a bilayer. In principle, this question should be easy to settle from the observed surface to bulk intensity ratio if no diffraction effects were present.

Pronounced diffraction effects were, however, revealed in the surface-to-bulk intensity ratio both as a function of kinetic energy and as a function of electron emission angle (see Figs. 5 and 6) and similar effects were observed earlier on Mo_3Si surfaces.[13] These diffraction effects prevent us from making a simple estimate of the amount of Si in the surface layers. When combined with theoretical calculations, photoelectron diffraction effects have been shown[28–30] to supply valuable structural information. Since the kinetic energies involved are low a full multiple-scattering calculation is needed and at present we cannot perform such calculations. Extension of this work into more detailed studies of the energy- and angle-dependent diffraction effects, including model calculations, and scanning tunnel microscope investigations for the purpose to extract information about relaxation effects and the structure of the terminating layers on these surfaces is planned.

V. SUMMARY AND CONCLUSION

Results of high-resolution angle-resolved core-level photoemission studies of the (100), (110), and (111) surfaces of Cr_3Si, cleaned by sputter and annealing cycles, have been reported. Surface-shifted Si $2p$ levels were revealed on all three surfaces while no surface shifted Cr $3p$ could be detected. A curve-fitting procedure using two shifted components on each surface was used in order to extract the surface shifted components. Shifts of -0.29 and -0.56 eV for the (100) surface, of -0.42 and -0.77 eV for the (110), and of -0.27 and $+0.28$ eV for the (111) surface were extracted. The origin of these shifts has been discussed.

The LEED pattern from the (100) surface indicated an overlayer structure, while the diffraction pattern from the other two surfaces were compatible with perfect bulk termination. The overlayer structure was suggested to be a two-domain $c(\sqrt{2}\times 2\sqrt{2})R45°$ structure consisting of Si.

Large differences in the oxidation rate were found for the different surfaces. All surfaces showed an initial rapid Si oxidation, while Cr oxidation could be detected first after considerably higher oxygen doses. That these surfaces are more reactive than pure Si and that they exhibit different oxidation rates is in agreement with earlier suggestions that the metal atoms acts as a catalyst to dissociate the oxygen molecules into more reactive atomic oxygen.

Distinct diffraction effects, both as a function of the photoelectron kinetic energy and electron emission angle, were observed in the surface-to-bulk intensity ratio. These effects prevented us from drawing any conclusions about the Si content in the terminating layers from measured surface to bulk intensity ratios.

ACKNOWLEDGMENTS

The authors would like to thank the staff at the MAX Laboratory for their support during the experiments and the Swedish Natural Science Research Council for their financial support.

[1]S. P. Murarka, *Silicides for VLSI Application* (Academic, New York, 1983).
[2]C. Calandra, O. Bisi, and G. Ottaviani, Surf. Sci. Rep. **4**, 271 (1985), and references therein.
[3]P. Wetzel, C. Pirri, J. C. Peruchetti, D. Bolmont, and G. Gewinner, Phys. Rev. B **35**, 5880 (1987).
[4]A. Franciosi, D. J. Peterman, J. H. Weaver, and V. L. Moruzzi, Phys. Rev. B **25**, 4981 (1982).
[5]P. Wetzel, C. Pirri, J. C. Peruchetti, D. Bolmont, and G. Gewinner, Surf. Sci. **178**, 27 (1986).
[6]C. C. Hsu, Baoqui Li, and Sunan Ding, Vacuum **41**, 690 (1990).
[7]A. Franciosi, J. H. Weaver, D. G. O'Neill, F. A. Schmidt, O. Bisi, and C. Calandra, Phys. Rev. B **28**, 7000 (1983).
[8]W. Speier, E. v. Leuken, J. C. Fuggle, D. D. Sarma, L. Kumar, B. Dauth, and K. H. J. Buschow, Phys. Rev. B **39**, 6008 (1989).
[9]F. Nava, T. Tien, and K. N. Tu, J. Appl. Phys. **57**, 2018 (1985).
[10]L. I. Johansson, K. L. Håkansson, U. O. Karlsson, and A. N. Christensen, Surf. Sci. **251/252**, 101 (1991).
[11]U. O. Karlsson, J. N. Andersen, K. Hansen, and R. Nyholm, Nucl. Instrum. Methods A **282**, 533 (1989).
[12]P. H. Mahowald, D. J. Friedman, G. P. Carey, K. A. Bertness, and J. J. Yeh, J. Vac. Sci. Technol. A **5**, (5), 2982 (1987).
[13]L. I. Johansson, K. L. Håkansson, P. L. Wincott, U. O. Karlsson, and A. N. Christensen, Phys. Rev. B **43**, 12 355 (1991).
[14]F. J. Himpsel, F. R. McFeely, A. Taleb-Ibrahimi, J. A. Yarmoff, and G. Hollinger, Phys. Rev. B **38**, 6084 (1988).
[15]G. Gewinner, J. C. Peruchetti, A. Jaegle, and A. Kalt, Surf. Sci. **78**, 439 (1978).
[16]G. Zajac, J. Zak, and S. D. Bader, Phys. Rev. B **27**, 6649 (1983).
[17]S. D. Bader, L. Richter, and T. W. Orent, Surf. Sci. **115**, 501 (1982).
[18]S. Valeri, U. Del Pennino, and P. Sassaroli, Surf. Sci. **134**, L537 (1983).
[19]A. Cros, R. A. Pollak, and K. N. Tu, Thin Solid Films **104**, 221 (1983).
[20]R. Leckey, J. D. Riley, R. L. Johnson, L. Ley, and B. Ditchek, J. Vac. Sci. Technol. A **6** (1), 63 (1988).
[21]F. J. Himpsel, B. S. Meyerson, F. R. McFeely, J. F. Morar, A. Taleb-Ibrahimi, and J. A. Yarmoff, in *Photoemission and Absorption Spectroscopy of Solids and Interfaces with Synchrotron Radiation,* "Enrico Fermi," Course CVIII, edited by M. Campagna and R. Rosei (North-Holland, Amsterdam, 1990), pp. 218 and 219.
[22]E. A. Wood, J. Appl. Phys. **35**, 1306 (1964).
[23]G. Hollinger and F. J. Himpsel, J. Vac. Sci. Technol. A **1**, (2), 640 (1983).
[24]A. Nilsson, B. Eriksson, N. Mårtensson, J. N. Andersen, and J. Onsgaard, Phys. Rev. B **38**, 10 357 (1988).
[25]T. Komeda, T. Hirano, G. D. Waddill, S. G. Anderson, J. P. Sullivan, and J. H. Weaver, Phys. Rev. B **41**, 8345 (1990).
[26]J. E. Rowe, G. K. Wertheim, and R. T. Tung, J. Vac. Sci. Technol. A **7** (3), 2454 (1989).
[27]A. Franciosi and J. H. Weaver, Phys. Rev. B **27**, 3554 (1983).
[28]H. C. Poon, G. Grenet, S. Holmberg, Y. Jugnet, Tran Minh Duc, and R. Leckey, Phys. Rev. B **41**, 12 735 (1990).
[29]Y. Jugnet, N. S. Prakash, L. Porte, Tran Minh Duc, T. T. A. Nguyen, R. Cinty, H. C. Poon, and G. Grenet, Phys. Rev. B **37**, 8066 (1988).
[30]R. A. Bartynski, D. Heskett, K. Garrison, G. Watson, D. M. Zehner, W. N. Mei, S. Y. Tong, and X. Pan, J. Vac. Sci. Technol. A **7** (3), 1931 (1989).

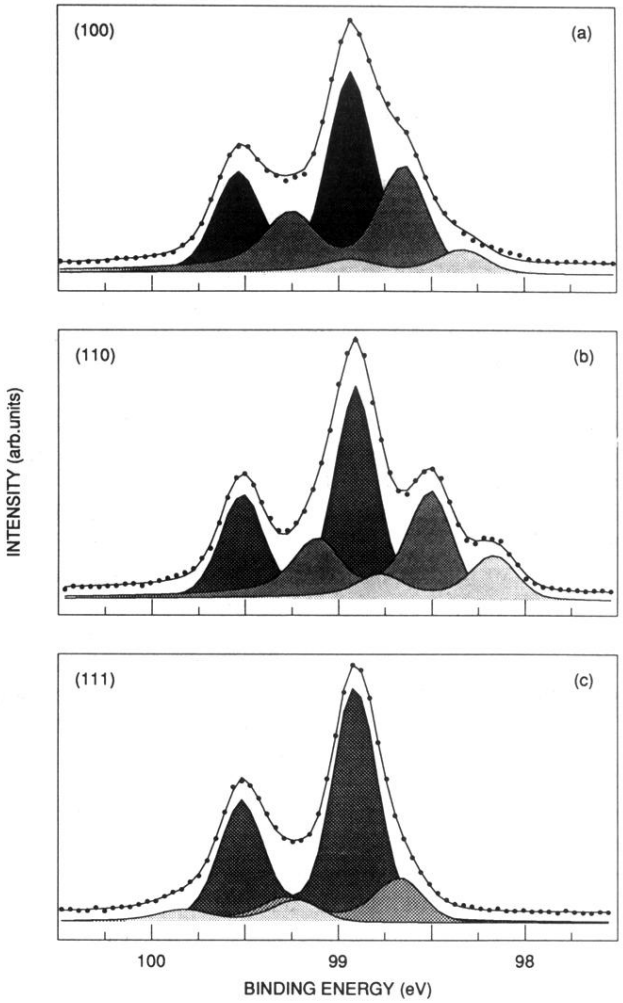

FIG. 2. Si 2*p* core-level spectra recorded at normal emission from (a) the (100) surface, (b) the (110) surface, and (c) the (111) surface using a photon energy of 130 eV. The dotted curves show the recorded data points, the solid curves represent the result of the curve fitting procedure, and the shaded curves show the extracted bulk (dark) and surface shifted (lighter) components.

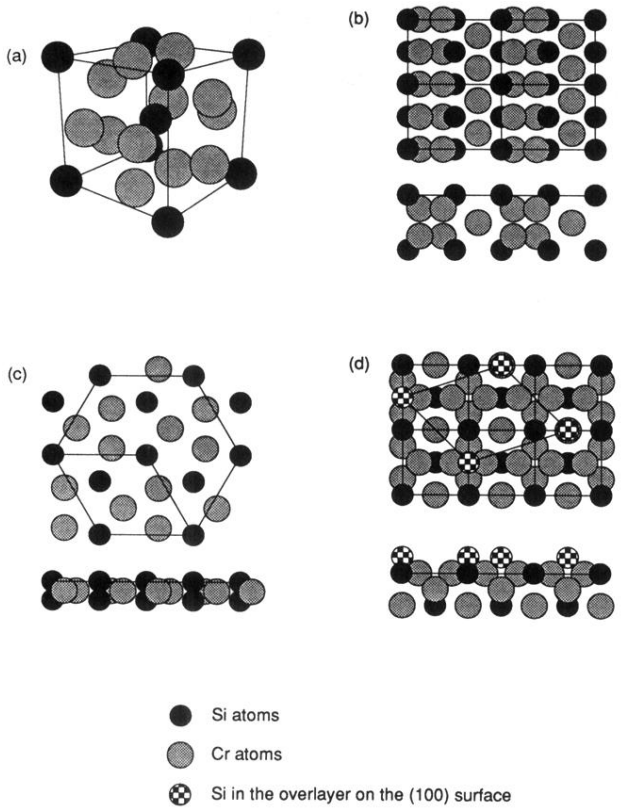

FIG. 7. (a) The unit cell of Cr_3Si where the large gray circles represents Cr atoms and the small black circles represents Si atoms. The top and side view of the low index surfaces are shown in (b)–(d) when assuming perfect bulk termination with Si in the surface layer for the (110) and (111) surfaces and a Si overlayer for the (100) surface.